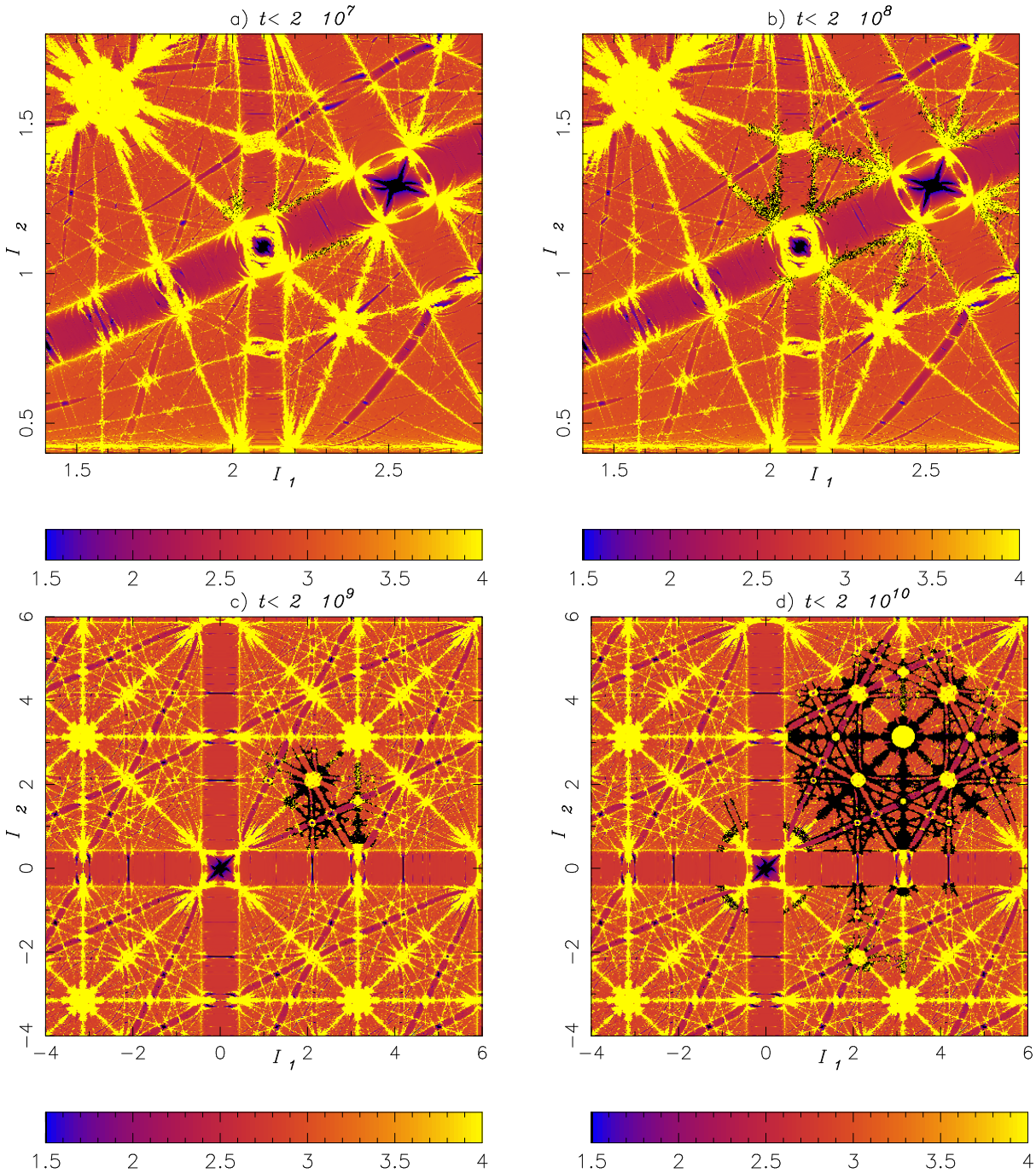

Figure 1. The four panels correspond to the FLI map of the action plane (I_1, I_2) for the map (2), with initial condition on the section S, with different magnifications. The light grey region corresponds to the chaotic part of the Arnold web. On panel (a,b,c,d) we mark with a black dot all points of the 90 orbits which have returned after some time on the section S. We consider $2\,10^7$ iterations for panel (a); $2\,10^8$ iterations for panel (b), $2\,10^9$ iterations for panel (c) and $2\,10^{10}$ iterations for panel (d).

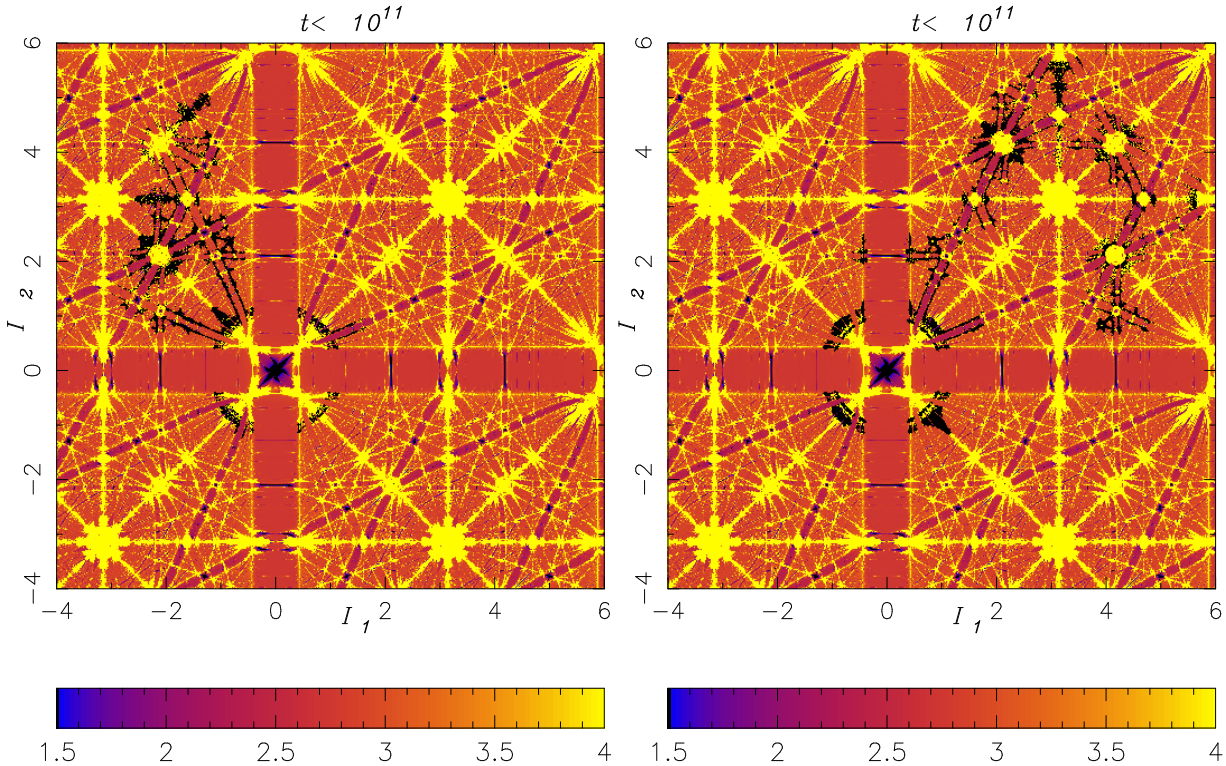

Figure 2. The two panels correspond to the FLI map of the action plane (I_1, I_2) for the map (2), with initial condition on the section S. The light grey region corresponds to the chaotic part of the Arnold web. The different panels correspond to the intersections with section S up to a time $t = 10^{11}$ of two orbits with initial conditions on the resonant line $I_1 = 2I_2$. More precisely, left panel represent the evolution of one orbit with initial conditions $I_1(0) = 1.71640$ and $I_2(0) = 0.8160$, while the right panel shows the evolution of one orbit with initial conditions $I_1(0) = 1.71643$, $I_2(0) = 0.8159$. Let us remark that although the initial conditions are very close the two orbits undergo completely different paths.

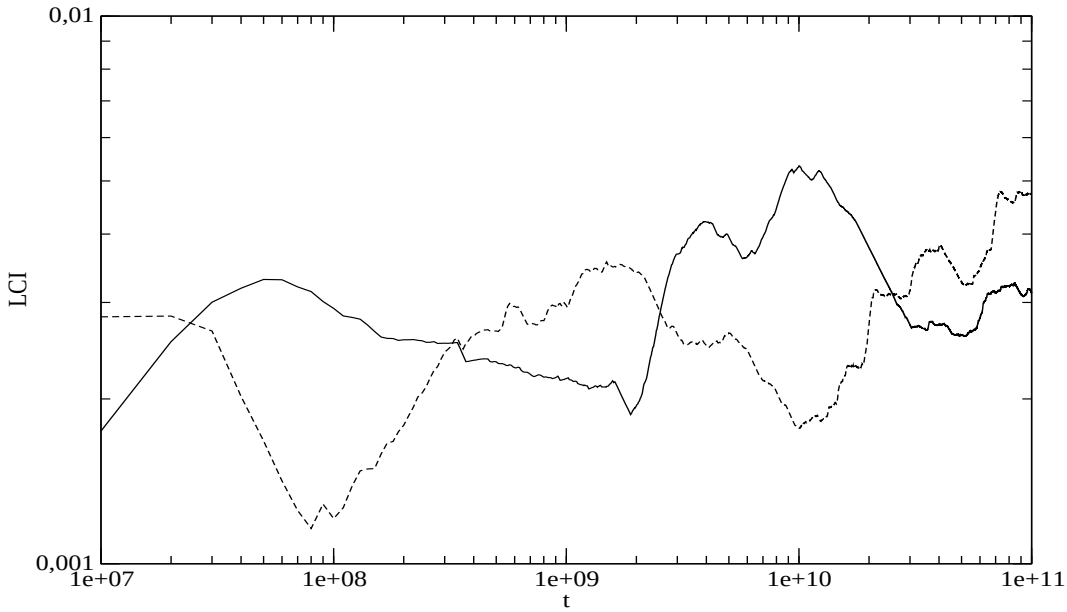

Figure 3. Evolution with time of the LCI of the two orbits of Fig.2

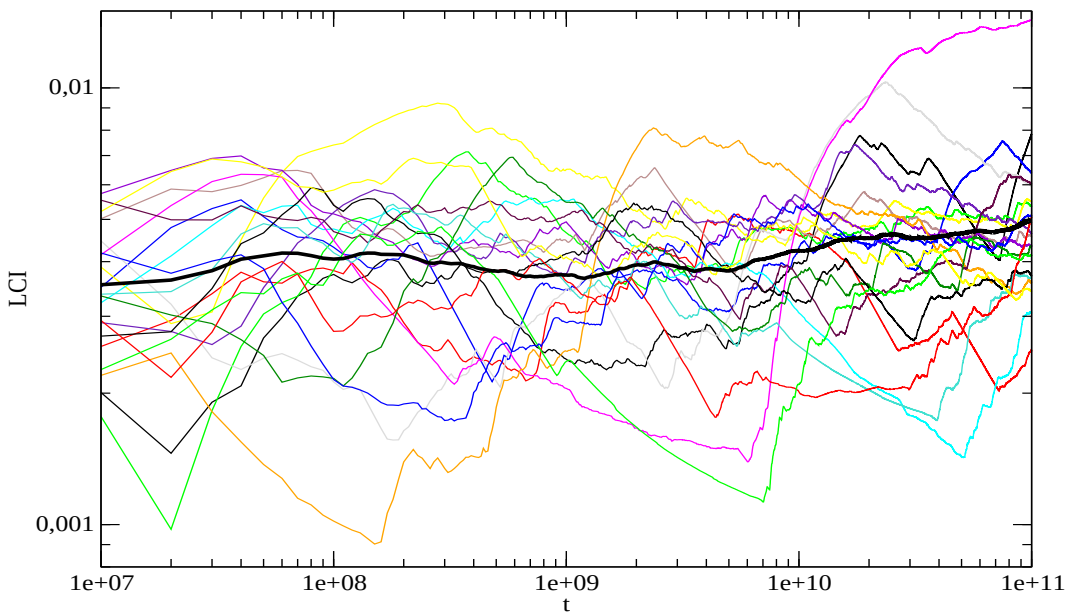

Figure 4. Evolution with time of the LCI of 20 of the 90 orbits of Fig.1. The more regular curve (thick line) is the evolution with time of mean value of the 90 LCI.

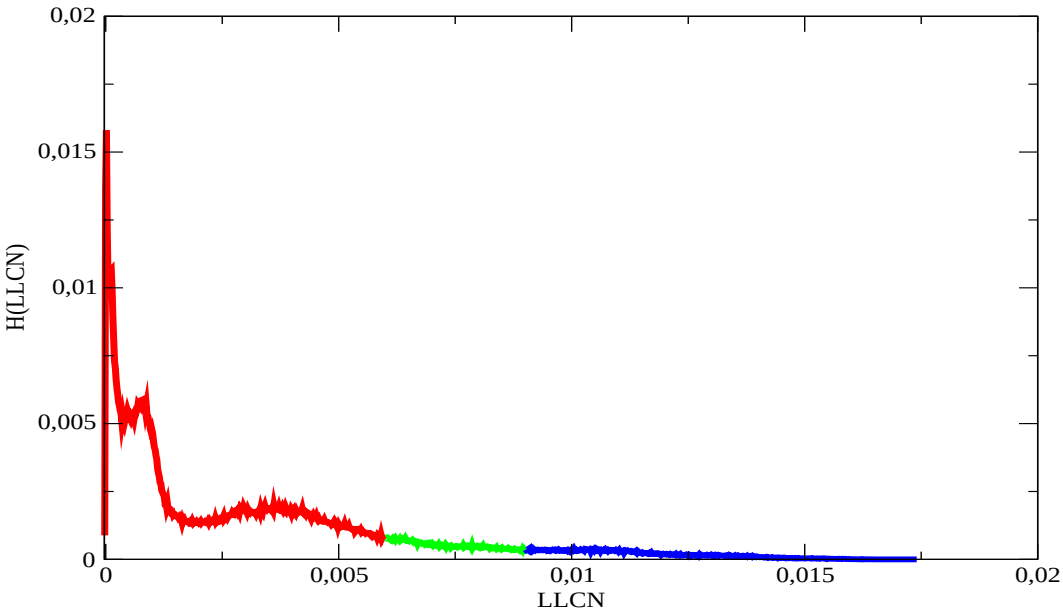

Figure 5. Distribution of the LLCNS of the orbit of Fig.2,left.

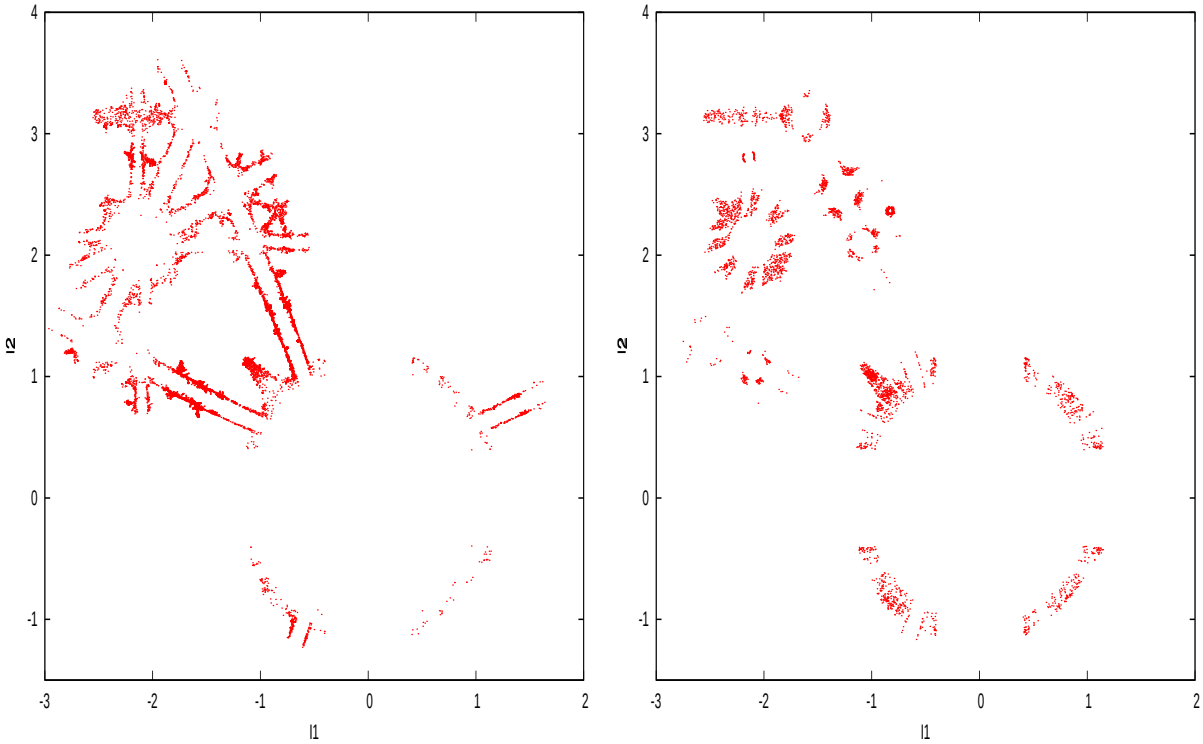

Figure 6. In the two panel the intersections of the point of the orbit of Fig.2 (left) with the section S are plotted. More precisely the points intersecting S and having $LLCN < 0.005$ are plotted in left panel the others in the right panel.

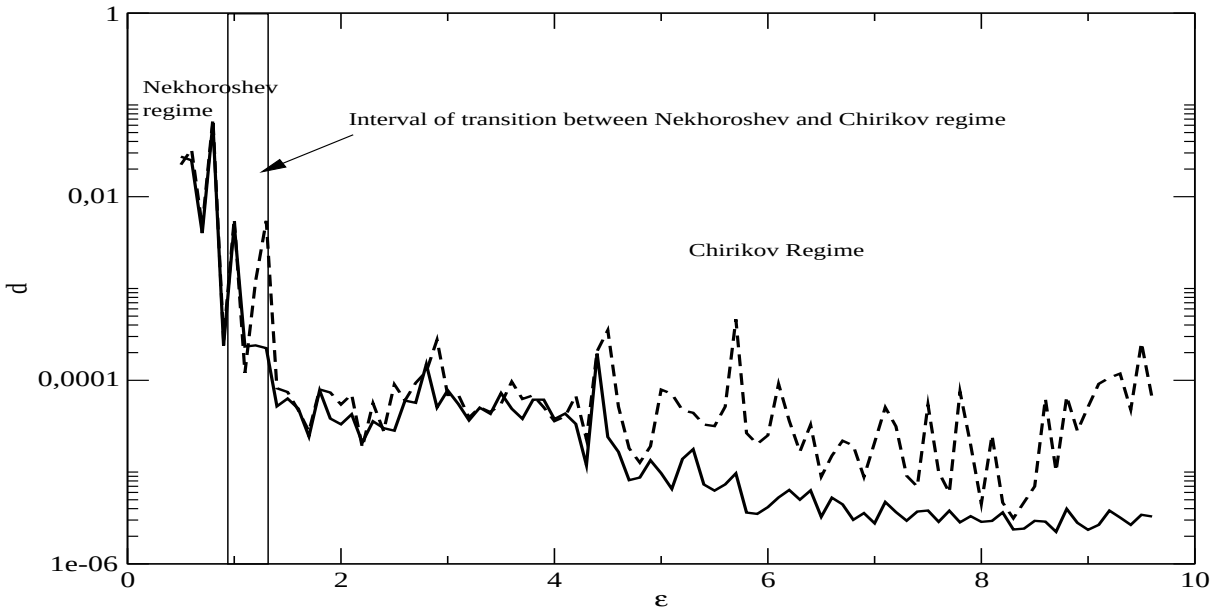

Figure 7. variation of the distance d as a function of ϵ. All points of data set 1 and data set 2 are considered (dashed line). Only 90 orbits of data set 1 and 90 sets of data set 2 having similar mean values of the LLCNs have been analyzed (continuous line). The interval $0.9 < \epsilon < 1.3$ correspond to the transition between the Nekhoroshev and the Chirikov regime.

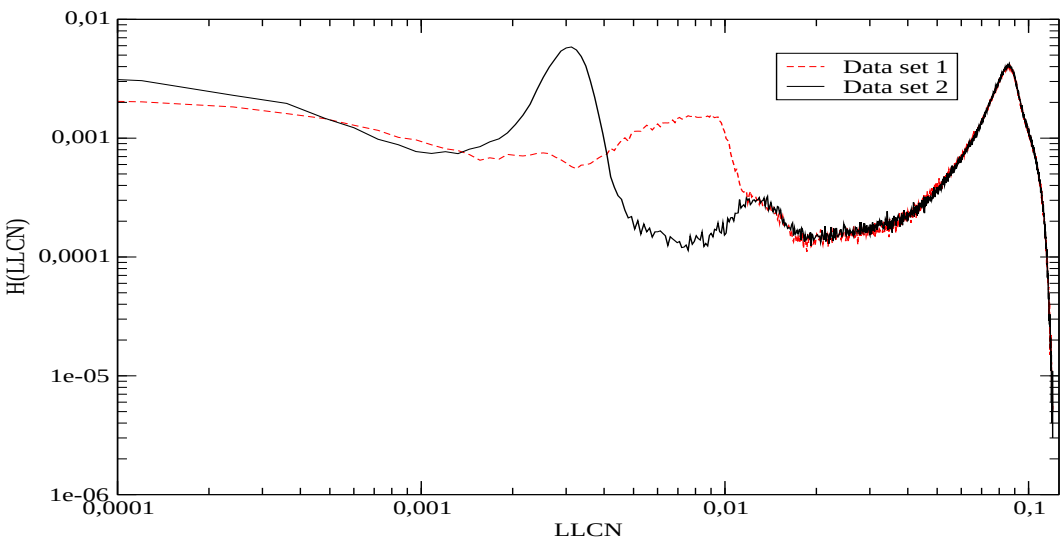

Figure 8. Histogram of the distribution of the LLCNs for data set 1 (100 orbits integrated for 10^8 iterations) and data set 2 (1 single orbit integrated for 10^{10} iterations).

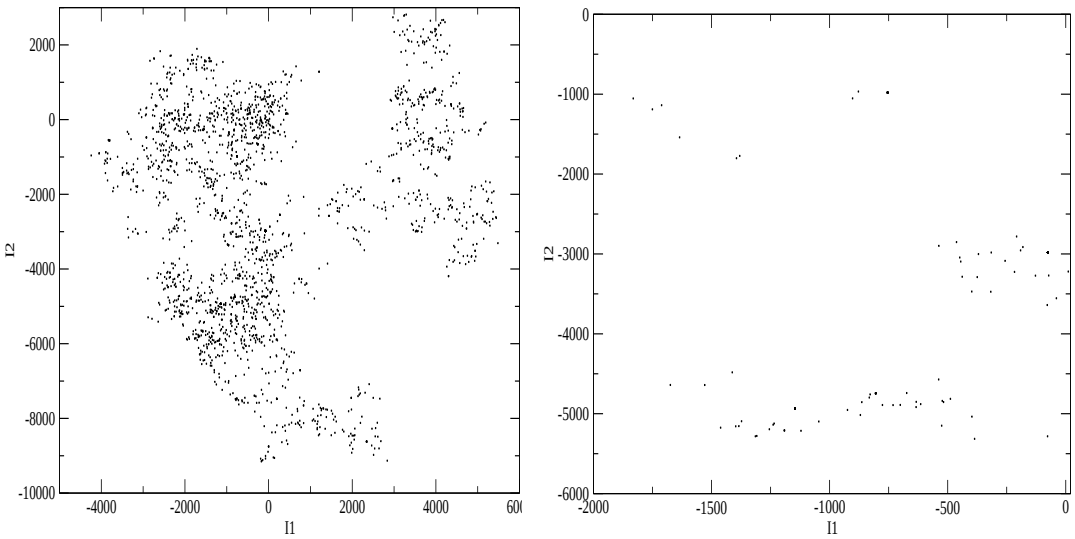

Figure 9. In the two panel the intersections of the point of the orbit of data set 2 with the section S are plotted. More precisely the points intersecting S and having $LLCN < 0.01$ are plotted in left panel the others in the right panel.

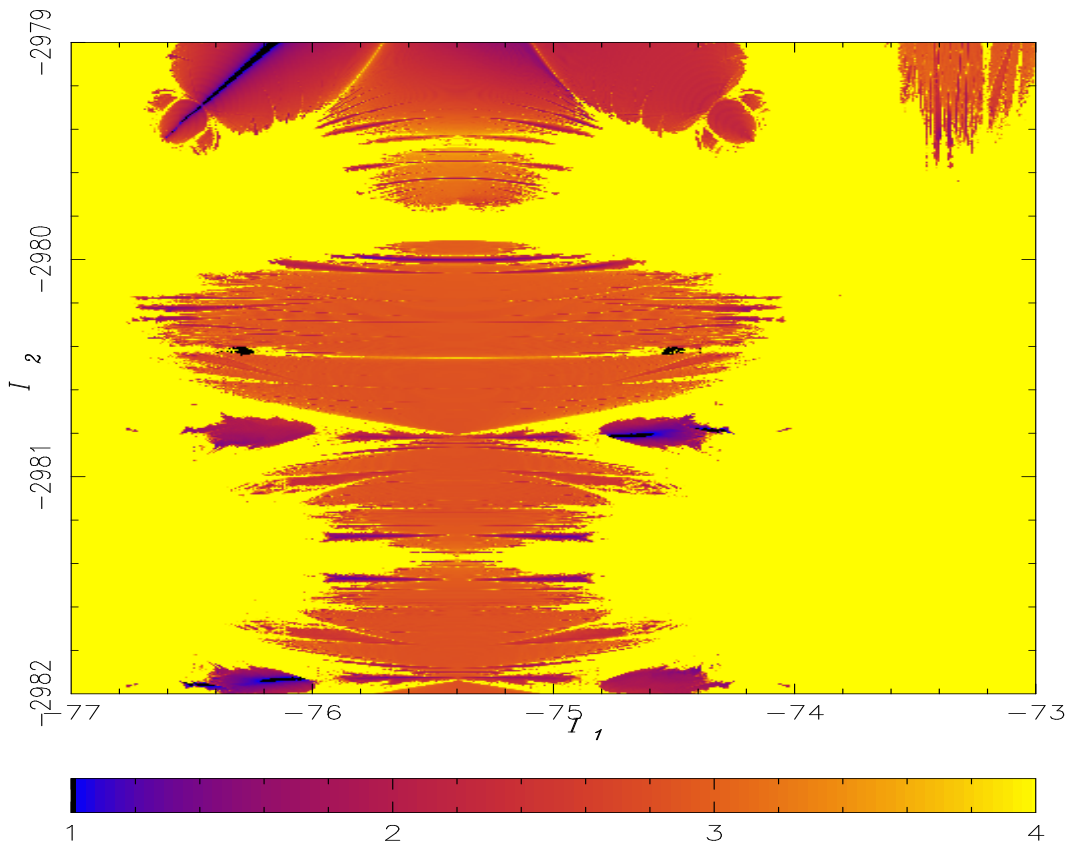

Figure 10. FLI chart of the zone of the phase space whit-in the box of Fig.9. The points of the orbit of data set 2 intersecting the section S and having LLCN<0.01 are plotted in black. They appear as two spots at about $I_2 \simeq -2980.5$ lying in a close neighbourhood of regular orbits.

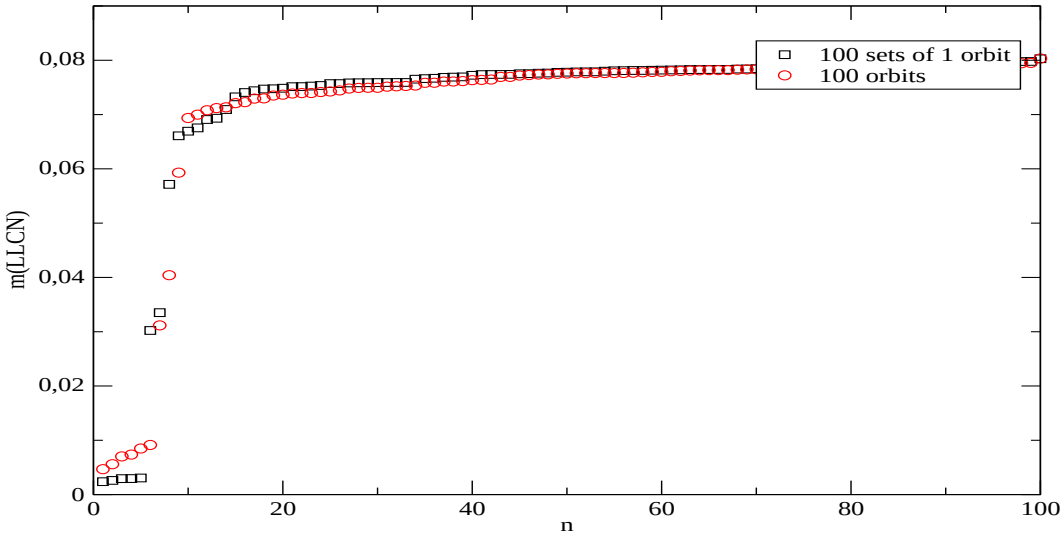

Figure 11. Mean values, ordered from minimum to maximum value, of the distributions of the LLCNs of the 100 orbits (data set 1) and of the 100 sets of 10^8 iterations of the single orbit (data set 2) for $\epsilon = 9.5$.

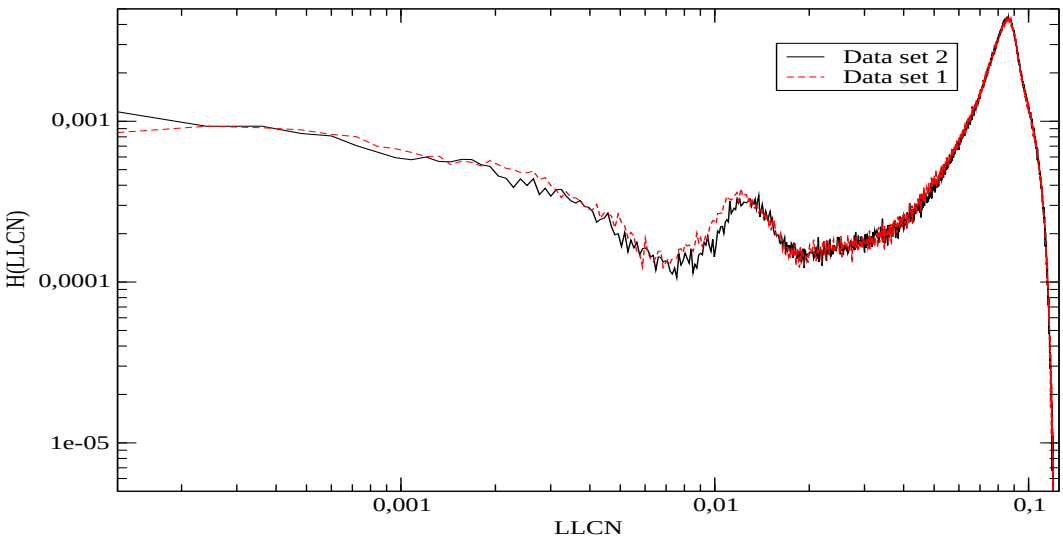

Figure 12. Histogram of the distribution of the LLCNs of data set 1 (90 orbits selected as explained in the text) and of data set 2 (90 sets of the single orbit selected as explained in the text).